Available online at www.sciencedirect.com
ScienceDirect
Applied Geochemistry 23 (2008) 419–437
Applied Geochemistry
www.elsevier.com/locate/apgeochem

Characterization and cycling of atmospheric mercury along the central US Gulf Coast

Mark A. Engle [a,*], Michael T. Tate [b], David P. Krabbenhoft [b], Allan Kolker [a], Mark L. Olson [b], Eric S. Edgerton [c], John F. DeWild [b], Ann K. McPherson [d]

[a] US Geological Survey, Eastern Energy Resources Team, 12201 Sunrise Valley Drive, MS 956, Reston, VA 20192, USA
[b] US Geological Survey, Wisconsin Water Science Center, Middleton, WI, USA
[c] Atmospheric Research and Analysis Inc., Cary, NC, USA
[d] US Geological Survey, Alabama Water Science Center, Montgomery, AL, USA

Available online 11 January 2008

Abstract

Concentrations of atmospheric Hg species, elemental Hg (Hg°), reactive gaseous Hg (RGM), and fine particulate Hg (Hg-$PM_{2.5}$) were measured at a coastal site near Weeks Bay, Alabama from April to August, 2005 and January to May, 2006. Mean concentrations of the species were 1.6 ± 0.3 ng m^{-3}, 4.0 ± 7.5 pg m^{-3} and 2.7 ± 3.4 pg m^{-3}, respectively. A strong diel pattern was observed for RGM (midday maximum concentrations were up to 92.7 pg m^{-3}), but not for Hg° or Hg-$PM_{2.5}$. Elevated RGM concentrations (>25 pg m^{-3}) in April and May of 2005 correlated with elevated average daytime O_3 concentrations (>55 ppbv) and high light intensity (>500 W m^{-2}). These conditions generally corresponded with mixed continental-Gulf and exclusively continental air mass trajectories. Generally lower, but still elevated, RGM peaks observed in August, 2005 and January–March, 2006 correlated significantly ($p < 0.05$) with peaks in SO_2 concentration and corresponded to periods of high light intensity and lower average daytime O_3 concentrations. During these times air masses were dominated by trajectories that originated over the continent. Elevated RGM concentrations likely resulted from photochemical oxidation of Hg° by atmospheric oxidants. This process may have been enhanced in and by the near-shore environment relative to inland sites. The marine boundary layer itself was not found to be a significant source of RGM.

Size segregation determination, using a limited dataset from two different methods, suggested that a significant fraction of particulate Hg was bound to coarse particles (>2.5 μm). A potential source of the large fraction of coarse particulate Hg in the study area is sequestration of RGM within sea salt aerosols. The presence of rapidly depositing RGM and coarse particulate Hg may be important sources of Hg input along the Gulf Coast. However, the impact of these species on deposition rates is yet to be determined.

1. Introduction

Atmospheric transport and deposition is an important pathway for the global distribution of Hg. Inputs to the ~5000 Mg global atmospheric

* Corresponding author.
E-mail address: engle@usgs.gov (M.A. Engle).

0883-2927/$ - see front matter © 2008 Published by Elsevier Ltd.
doi:10.1016/j.apgeochem.2007.12.024

Hg pool (Mason et al., 1994) include both natural (e.g., soils, vegetation, volcanoes, fires, mineral deposits; Ferrara et al., 2000; Gustin, 2003; Friedli et al., 2003) and anthropogenic sources (e.g., coal combustion, waste incineration, and chlor-alkali production; Schroeder and Munthe, 1998; Fitzgerald and Lamborg, 2005). Transport of atmospheric Hg from these sources to the surface via wet and dry deposition dominates Hg input to some ecosystems (Krabbenhoft et al., 2005; Hines and Brezonik, 2007). Once in the natural environment, inorganic Hg may be converted to an organic form, such as methylmercury, typically through biomediated reactions (Paterson et al., 2006). Methylmercury is a neurotoxin that has the potential to bioaccumulate and biomagnify through the food web (Zillioux et al., 1993; Morel et al., 1998). The importance of atmospheric Hg deposition on ecosystem response has been highlighted by field-based studies in the Florida Everglades (Krabbenhoft et al., 2004) and a boreal forest watershed in Canada (Hintelmann et al., 2002; Branfireun et al., 2005) linking additions of inorganic Hg in wet deposition to increased methylmercury production. However, a direct relationship between Hg deposition and methylmercury production is not universally established and requires further examination (Fitzgerald et al., 1998).

Atmospheric Hg is typically categorized as three species: elemental Hg (Hg°), reactive gaseous mercury (RGM), and particulate Hg (Hg-P). Roughly 95% of the Hg in the troposphere occurs in the Hg° state; RGM and Hg-P typically make up the remaining 5% (Schroeder and Munthe, 1998). Gaseous Hg° is generally unreactive, sparingly soluble, and thought to exhibit a low dry deposition velocity (0.02–0.2 cm s^{-1}; Xu et al., 1999; Poissant et al., 2004; Seigneur et al., 2004) allowing it to be transported a significant distance from its original source (Jaffe et al., 2005; Seigneur et al., 2004). Reactive gaseous Hg species, assumed to be Hg(II) and possibly Hg(I)-bearing gaseous compounds (e.g., $HgCl_2$, $HgBr_2$, HgO, etc.), have significantly higher deposition velocities than Hg° (0.4–7.6 cm s^{-1}; Poissant et al., 2004; Marsik et al., 2007) and are thought to be readily bioavailable (Lindberg et al., 2002). Particulate Hg also has a relatively high deposition rate and can be transported regionally (500–800 km), depending on particle size (Keeler et al., 1995; Wängberg et al., 2003). Gaseous Hg° can be converted to RGM and/or Hg-P via reactions with atmospheric oxidants such as O_3, $OH^{\bullet}$, and halogen radicals, such as $BrO^{\bullet}$ (Calvert and Lindberg, 2005: Pal and Ariya, 2004a,b; Sommar et al., 2001). Reactive gaseous Hg and Hg-P can deposit faster, over a more local range than Hg°, due to higher solubility and dry deposition rates.

Wet deposition of Hg at Mercury Deposition Network sites in states bordering the Gulf of Mexico (i.e., Florida, Alabama, Mississippi, Louisiana and Texas) is elevated (up to 27 μg m^{-3} a^{-1}) relative to other regions in the US (typically <15 μg m^{-3} a^{-1}; Mercury Deposition Network, 2006). High wet deposition rates along the Gulf Coast correlate with high annual precipitation (~1000–2000 mm a^{-1}) and moderate to above average precipitation Hg concentrations (8.5–16.4 ng L^{-1}; Mercury Deposition Network, 2006). Source apportionment studies in the Florida Everglades, part of the US Gulf Coast region, concluded that local industrial sources (e.g., waste incinerators) were the dominant source of Hg in aerosols and precipitation (Dvonch et al., 1998; Guentzel et al., 2001). Other researchers, however, argued that long-range transport of RGM and scavenging of Hg during convective thunderstorms is the dominant source of Hg in wet deposition of southern Florida, rather than local source input (Guentzel et al., 1998, 2001). In an attempt to better understand and assess potential mechanisms and/or sources controlling elevated wet deposition in the Gulf Coast region, research presented here characterizes and examines the cycling of atmospheric Hg in the vicinity of Mobile Bay, Alabama (Fig. 1).

Characterization of atmospheric Hg speciation has been previously investigated at coastal sites in Florida and Maryland (Malcolm et al., 2003; Laurier and Mason, 2007). The RGM concentration data presented in these studies typically followed a diel pattern of low concentrations at night, increasing in mid-morning to a midday maximum, then decreasing into the evening. This diel pattern is typical of photochemically derived chemicals, such as HO_2 (Seinfeld and Pandis, 2006). Peaks in RGM concentration at these sites typically corresponded with non-marine air flows, often during stagnant conditions, rather than marine air. These results differ greatly from elevated RGM measurements taken over the open ocean during low O_3 (<30 ppbv) conditions, which implicate Hg° oxidation by halogen radicals, generated from sea salt aerosols, as the likely source (Hedgecock et al., 2003, 2005; Sheu and Mason, 2004). Laurier and Mason (2007) suggested that in situ photochemical formation of

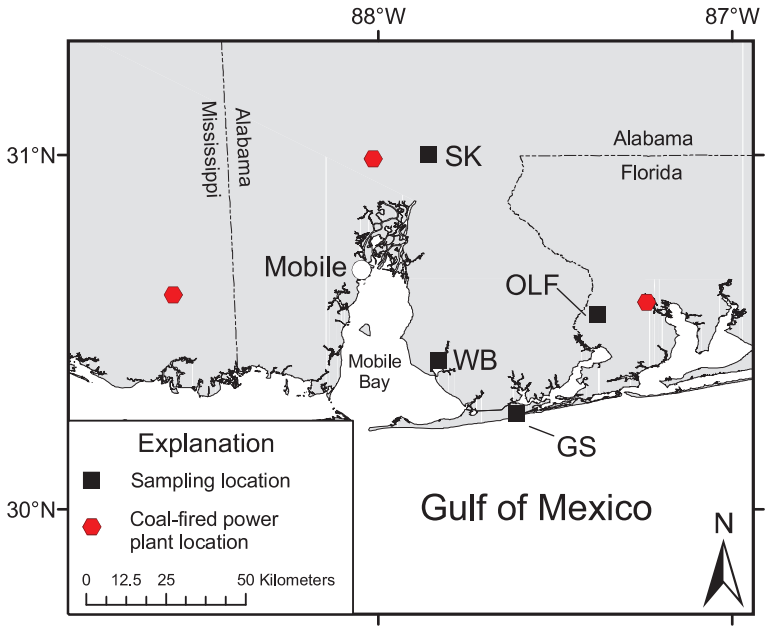

Fig. 1. Map showing locations of sampling sites, coal-fired power plants, and metropolitan areas in the study area. GS = Gulf Shores, WB = Weeks Bay, SK = Stockton, and OLF = Outlying Landing Field.

RGM may also occur in coastal environments but higher O_3 concentrations and air temperature in these settings may limit halogen-based Hg° oxidation reactions. Malcolm et al. (2003) also compared fine particulate Hg (Hg-$PM_{2.5}$) and total suspended Hg (Hg-TSP) measurements at a coastal site in Florida and concluded that a significant fraction of particulate Hg was bound to large particles, such as sea salt aerosols. Given the high solubility and potentially rapid deposition rate of Hg-bearing sea salt aerosols and RGM compounds, these limited findings have implications for atmospheric Hg deposition in coastal settings. Despite work presented in these previous studies, significant questions remain about the spatial and temporal variability of RGM concentrations, the importance of Hg bound to large aerosols, and dominant controls on atmospheric Hg cycling in coastal environments.

In an attempt to address questions raised by previous research, the objectives for this paper were to (1) characterize concentrations of atmospheric Hg species at a coastal site along the Alabama Gulf Coast region for a ~1-a period; (2) link trends in the Hg speciation data with changes in physical, chemical, and meteorological conditions, to identify potential sources and sinks of atmospheric Hg species; (3) quantify Hg and trace elements in total suspended particulate samples; and (4) determine the relative importance and association of Hg bound to coarse (>2.5 μm) aerosols. Findings from this investigation are discussed in terms of better understanding the behavior and cycling of atmospheric Hg in the central US Gulf Coast region.

2. Description of regional meteorology, sampling sites, and field sampling strategy

Meteorology of the central US Gulf Coast is strongly controlled by high solar intensity, warm temperatures, high relative humidity, and proximity to the Gulf of Mexico. Several patterns of atmospheric circulation are present in the region, most notably a continental high where cool, dry air is transported down from Canada; a Gulf return system which brings in tropical air from the Caribbean; and a Gulf high which carries maritime air along with drier continental air from Texas or Mexico into the region (Muller, 1977). Sea-breeze circulation, which is driven by thermal differences between the land and sea, dominates wind patterns locally and can lead to the development of convective storms. This circulation phenomenon allows for frequent shifts from onshore flow to offshore flow and the reverse, often over a daily time step, depending on cooling and heating patterns (Rogers, 1995). Offshore flow can trap continentally-derived atmospheric pollutants and their precursors in the shallow marine boundary layer, only to later return during a shift to onshore

flow (Hanna, 1991). The rainy season, lasting from May to October, brings thunderstorms, tropical storms, and occasionally hurricanes from the Gulf of Mexico and provides a significant contribution to the area annual average precipitation of roughly 1600 mm (Ning and Abdollahi, 2003). Meteorological conditions during the cool season (February–March) are characterized by Canadian cold, dry air masses from the land tracking over the sea, increasing in humidity and temperature, and returning to the continent (Muller, 1977). These processes add complexity to understanding central Gulf Coast atmospheric chemistry and cycling.

To examine the influence of the near-shore marine atmospheric environment with more inland influences, the sites were placed at varying distances to the coastline (Fig. 1). They include Weeks Bay (WB), Gulf Shores (GS) and Stockton (SK) in Alabama and Outlying Landing Field (OLF), Florida. The WB site is a ~100 m diameter, open field surrounded by a deciduous canopy at the Weeks Bay Natural Estuarine Research Reserve. The site is roughly 500 m north of Weeks Bay, a small embayment that flows into the salt-water dominated Mobile Bay. The WB site is located 35 km SE of Mobile, Alabama, a medium-sized industrial city (metropolitan area population = 400,000). The GS site is located in a clearing on the north side of Shelby Lakes lagoon within Gulf Shores State Park, less than 1 km from the Gulf of Mexico. The area around the GS site consists of limited residential and commercial development. Queries of the US Environmental Protection Agency's Toxic Release Inventory database (http://www.epa.gov/triexplorer/) provided no evidence of significant trace element sources within 50 km of the site. The SK site was established on a 200 m × 200 m open field in a rural forested inland setting roughly 40 km NE of Mobile. A large (1800 MW) coal-fired power plant is located roughly 20 km west of the SK site and is a potential source of Hg, SO_2, and other pollutants. The fourth site (OLF), located in a suburban airshed ~20 km NW of Pensacola, Florida (metropolitan area population = 437,000), is roughly 15 km west of another coal-fired power plant (Fig. 1). The OLF site is a long-term research site for atmospheric Hg, particulate matter and O_3, operated by Atmospheric Research & Analysis Inc. Additional information about the OLF site is given by Edgerton et al. (2006).

The USGS mobile Hg laboratory was deployed at the WB site with the goal of characterizing atmospheric Hg speciation (Hg°, RGM, Hg-$PM_{2.5}$) and monitoring meteorology and O_3, NO_x and SO_2 concentrations. The lab was operated from April 13, 2005 until August 29, 2005, when the trailer housing the instrumentation (described below) was severely damaged during Hurricane Katrina. A new trailer containing the original analyzers was deployed to the site on January 4, 2006 and continued to operate through May 21, 2006.

Total suspended particulate (TSP) sampling at WB and GS was conducted from April 14–21, 2005 and at the WB, GS and SK sites from June 7–16, 2005 (Table 1). Total suspended particulate sampling at the WB site overlapped with operation of the USGS mobile Hg laboratory, allowing for comparison of Hi-Vol and Low-Vol TSP results with speciated measurements during the April and June sampling periods. Two types of samplers were used to collect the aerosol samples: low-volume TSP (Low-Vol) and high-volume TSP (Hi-Vol), as described below. Distribution and sampling information on the samplers are provided in Table 1.

Speciated atmospheric Hg measurements (Hg°, RGM, Hg-$PM_{2.5}$) were also made at the OLF site,

Table 1
Collection period, sampling rate, and targeted analytes of atmospheric Hg speciation system, Low-Vol TSP and Hi-Vol TSP samplers and their deployments during the April 2006 and June 2006 TSP sampling periods

Sampler	Analytes	Collection period	Sampling rate	April 14–21, 2005		June 7–16, 2005		
				GS	WB	GS	WB	SK
Atmospheric Hg speciation unit	Hg°	5 min	1.5 lpm		X		X	
	RGM	1 h	10 lpm		X		X	
	Hg-$PM_{2.5}$	1 h	10 lpm		X		X	
	Hg, Se, Al, Mg	12 h[a]	~30 lpm	X	X	P	X	P
Hi-Vol TSP sampler	Hg, $C1^-$, SO_4^{2-}	12 h	~1500 lpm	P	P	X	X	X

GS = Gulf Shores, WB = Weeks Bay, SK = Stockton, X = individual sampler employed throughout sampling period, P = individual sampler employed through a portion of the sampling period.

[a] Two sets samples from April at the WB site were collected over a 36-h period.

Table 2
Summary of inlet experiments at the OLF site

Experiment	Dates	Inlet		Hg°		Hg-P		RGM		n
		1	2	1	2	1	2	1	2	
Precision 1	October, 2005	$PM_{2.5}$	$PM_{2.5}$	1.57 (0.18)	1.60 (0.18)	0.83 (0.82)	1.85* (1.01)	5.35 (9.35)	4.91 (8.80)	84
TSP	October, 2005	$PM_{2.5}$	none	1.50 (0.09)	1.51 (0.27)	2.29 (2.00)	6.90 * (3.64)	4.85 (6.92)	5.75 (13.94)	83
Precision 2	April–May, 2006	$PM_{2.5}$	$PM_{2.5}$	1.45 (0.16)	1.52* (0.16)	1.88 (2.12)	1.75 (5.46)	5.43 (13.19)	4.95 (14.26)	230
PM_{10}	April–May, 2006	$PM_{2.5}$	PM_{10}	1.48 (0.12)	1.59* (0.12)	1.58 (2.28)	4.54* (4.32)	2.97 (10.8)	3.36 (13.32)	144

Mean concentrations with standard deviation in parentheses. Units for Hg° are ng m^{-3}; units for RGM and Hg-P species are pg m^{-3}. 1 = primary atmospheric Hg speciation system; 2 = collocated secondary atmospheric Hg speciation system; n = number of valid 60-min averages.

* Concentrations significantly ($p < 0.01$) greater than results from collocated atmospheric Hg speciation system unit.

during sampling periods in October, 2005 and April–May, 2006 (Table 2). Two separate collocated atmospheric speciation units were used, allowing direct comparison of different Hg size fractions. No other data collected at the OLF site are presented in this paper.

3. Methods

3.1. Automated atmospheric mercury speciation measurements

Atmospheric Hg speciation systems were deployed with the USGS mobile Hg laboratory at the WB site ($n = 1$ unit); results from 2 other units that operate as part of the Southeastern Aerosol Research and Characterization (SEARCH) program at the OLF site were also used in this study. The systems utilize a Tekran 1130/1135 speciation unit coupled to a Tekran 2537A Cold Vapor Atomic Fluorescence Spectrometer (CVAFS). The units, which are described in detail by Landis et al. (2002) and Lindberg et al. (2002), sequentially collect RGM on a KCl-coated annular denuder, fine particulate Hg (particle diameter <2.5 μm; Hg-$PM_{2.5}$) on a regenerable particulate filter and Hg° on Au traps. The collected Hg is thermally desorbed and analyzed by the Tekran 2537A as Hg°. Every 2 h the atmospheric Hg speciation system provides 12 consecutive 5-min average Hg° concentrations and 1-h integrated Hg-$PM_{2.5}$ and RGM concentrations.

The atmospheric Hg speciation system has an Hg° detection limit of approximately 0.1 ng m^{-3}, which is less than any of the Hg° measurements from this study. A detection limit for RGM and Hg-$PM_{2.5}$ of 1.5 ± 0.5 pg m^{-3} was calculated for this study. Roughly 42% of the Hg-$PM_{2.5}$ and 54% of the RGM data from this study were below the 1.5 pg m^{-3} detection limit.

The Tekran 2537A analyzer was calibrated monthly at WB and every 3 days at OLF using an internal permeation tube, which was periodically checked by injecting known quantities of elemental Hg. Calibrations produced an average $-5 \pm 8\%$ change in Hg° concentration at WB. Recovery of Hg° from manual injections made into both ambient air and Hg/oxidant free air at WB averaged 112.6% and ranged from 106.9% to 117% ($n = 14$). Variation in percent Hg° recovery between the two Au traps in the WB Tekran 2537A during manual injections ranged from 1.1% to 3.6%. The atmospheric Hg speciation systems at the OLF site provided similar calibration results, as presented in Edgerton et al. (2006). Standards do not currently exist for RGM and Hg-$PM_{2.5}$ but precision of the measurements is approximately 15–20% (Landis et al., 2002; Malcolm and Keeler, 2007). The annular denuder and regenerable particulate filter were replaced bi-weekly to monthly. A soda lime trap, used to avoid passivation of the two Au traps, was replaced weekly.

In addition to Hg analysis at the WB site, O_3, NO_x and SO_2 were analyzed using Thermo-Environmental models 49C, 43C and 42C, respectively. The O_3, NO_x, and SO_2 analyzers were calibrated monthly and operated within a 5% error margin. Inlets to the Hg speciation unit and oxidant analyzers at WB were located at roughly 4 m above the ground surface. Air temperature, precipitation, light intensity, wind direction and wind speed data were

collected and stored at 5-min intervals using a Campbell Scientific data logger; relative humidity was collected at 1-h intervals.

3.2. Aerosol sampling

Both Hi-Vol and Low-Vol TSP samplers were employed during this study (Table 1). The two sampling techniques varied in inlet height (1.1 vs. 2.0 m; Hi-Vol vs. Low-Vol), flow rate (1500 L min^{-1} vs. 30–35 L min^{-1}), filter orientation (upward facing vs. downward facing), and filter area (500 cm^2 vs. 17 cm^2). The two USGS-designed dual-head Low-Vol sampling stations were individually distributed between the GW, WB, and SK sites (Table 1). The Low-Vol TSP units had the capacity to sample through two acid-cleaned 47-mm open-faced filter packs (URG Corp.) at the same time, allowing for simultaneous collection of aerosols for trace element (1.2 μm pore size PTFE filters, Sartorius Inc.) and Hg analysis (pre-fired Millipore® quartz fiber filters, model AQF04700). Sampling was conducted over continuous day/night 12-h periods; filter packs were changed at approximately 6AM–8AM and 6PM–8PM, except for two sets of 36-h samples (Table 1). The sampling flow rate was measured at the beginning and end of each sampling period using a mass flow meter (Sierra Instruments Top-Track Model 820) and checked against dry gas meters (Hi-Q Model SK25). After sampling, the filters were placed in acid-cleaned air tight 50 mm diameter Petri dishes, which were sealed in individual polyethylene bags and frozen at −15 °C. Ultra-clean methods were employed during handling of the filters and filter packs.

The PTFE filters were digested in aqua regia at 85 °C. The digestion solution was analyzed for trace elements via ICP-AES, ICP-MS, and hydride generation AA at the USGS Central Energy Team Laboratories in Denver, Colorado (Garbarino et al., 2006). The quartz fiber filters were digested in a 5% BrCl solution at 50 °C for 5 days. The digest was analyzed for total Hg using cold vapor atomic fluorescence spectrometry (CVAFS) at the USGS Wisconsin District Mercury Laboratory in Middleton, Wisconsin (Olund et al., 2004).

Field blanks for Hg and trace elements consisted of new filters that were loaded into acid-cleaned PTFE filter packs, brought to one of the sampling sites, placed on the sampling tripod for roughly 10 min, and transferred to the filter's original Petri dish. Method detection limits (MDL) were calculated for each element as three times the standard deviation of field blanks ($n = 7$ for Hg, $n = 6$ for TM). The MDL for Low-Vol Hg results was 1.5 pg m^{-3} (blanks = 4.3 ± 12.6 pg $filter^{-1}$). Trace element results from Low-Vol sampling presented in this study are limited to Se (MDL = 1.0 ng m^{-3}), Al (MDL = 32.9 ng m^{-3}) and Mg (MDL = 3.5 ng m^{-3}). All laboratory results were blank corrected. Trace element results for five pairs of replicate Low-Vol PTFE filter sets were found to be not statistically different ($p < 0.05$, Wilcoxon sign rank test). Comparison of replicate Hg-TSP samples was not performed during this study. However, Low-Vol Hg-TSP results for a coastal area in South Carolina using the same sampling and analytical methods (Engle, unpublished data) produced an average difference between paired samples of 0.9 ± 0.6 pg m^{-3} or 17.0% ± 15.2% ($n = 14$ pairs).

The Hi-Vol TSP samplers (Tisch model TE-5000) collected aerosols over 12-h periods, comparable to those used for the Low-Vol samplers (Table 1). The flow of the TSP samplers was calibrated at the beginning and end of each sampling period using a fixed orifice calibrator (Tisch Model 5025A). Aerosols were collected on a pre-fired 20 cm × 25 cm quartz fiber filter. Filters were handled using ultra-clean methods. Field blanks consisted of filters which were placed on the sampler for roughly 2 min, while the pump was turned off. Method detection limits were calculated in a method similar to that used for the Low-Vol filters. After sampling, the used filters were folded in half to prevent material collected on the filters from rubbing off. Filters were stored in individual polyethylene bags at −15° C. Prior to analyses, the Hi-Vol filters were cut into quarter sections. One quarter was analyzed for total Hg using CVAFS, as described above (Hi-Vol Hg-TSP MDL = 3.2 pg m^{-3}). Soluble anions were extracted from the second quarter by soaking in 15 mL of nanopure water. A 5 mL aliquot of this extract was analyzed for Cl^- (MDL = 7.7 ng m^{-3}, $n = 8$ field blanks) and SO_4^{2-} (MDL = 8.5 ng m^{-3}, $n = 8$ field blanks) using liquid chromatography at the USGS Biogeochemistry Laboratory in Reston, Virginia. A portion of the remaining quarter sections from 16 Hi-Vol filters was examined for particle identification using microbeam methods, with a JEOL8900R electron microprobe analyzer at the USGS microbeam labs in Reston, Virginia. No particles were observed during microbeam analysis on filters collected as field blanks.

3.3. Size distribution of particulate Hg

To examine the size distribution of Hg-P, two independent methods were utilized. At the WB site, Hg-TSP results from adjacent Hi-Vol and Low-Vol samplers were compared with corresponding 12-h average Hg-$PM_{2.5}$ concentrations measured at the mobile lab. Differences between Hg-TSP and Hg-$PM_{2.5}$ concentrations were attributed to Hg-P bound to coarse fractions, although potential for sampling artifacts also had to be considered (as discussed in Section 4). At the OLF site, size distribution of aerosols was determined by comparing Hg-$PM_{2.5}$ results from one atmospheric Hg speciation system with corresponding Hg-PM_{10} or Hg-TSP concentrations from the other speciation unit. In addition, precision experiments were run to examine analytical differences between the two atmospheric Hg speciation units when both were using a $PM_{2.5}$ inlet.

3.4. Backward air mass trajectory modeling using HYSPLIT

To investigate potential source areas of Hg and other trace elements, the NOAA hybrid single-particle Lagrangian integrated trajectory model (HYSPLIT) using EDAS 40 km input data, was used to back-calculate air mass trajectories. The HYSPLIT model was accessed and run both through the NOAA website (http://www.arl.noaa.gov/ready/hysplit4.html) and a local installation on a personal computer. HYSPLIT air mass back-trajectory modeling for heights of 100 m, 250 m, and 500 m above the ground surface at the sites was completed during periods of daily maximum RGM concentrations during sampling in 2005 and 2006 and for every 4 h throughout the aerosol sampling events. Based on these results, trajectories were classified as one of three flow regimes: continental (dominated by terrestrial sources), Gulf (dominated by marine sources), or mixed (air masses traversing over both the Gulf and the continent). Aerosol samples collected during periods of different trajectory regimes (e.g., Gulf during the first 8 h and mixed during the last 4 h), and for the two 36-h Low-Vol aerosol samples were not categorized. Robustness of the HYSPLIT model was evaluated by comparing results between the trajectories for heights of 100 m, 250 m and 500 m and between modeling runs for every 4 h during the 12-h aerosol sampling period.

3.5. Statistical analyses

All statistical analyses were completed using NCSS version 2004 (Hintze, 2005). Given the non-normal distribution of most of the elements/species, robust and non-parametric statistical methods were applied. Comparison of statistical significance in terms of attribute magnitude was completed using Wilcoxon rank sum and Wilcoxon sign ranks test for unpaired and paired data, respectively. The Spearman rank method was used for all correlation calculations. All data were transformed in order to minimize effects of outliers and skewed data prior to regression analyses. Statistical significance is indicated at $p < 0.05$.

4. Results

4.1. Mercury speciation and atmospheric chemistry results

Elemental Hg concentrations measured at WB (1.62 ± 0.25 ng m^{-3}, $\bar{x} \pm \sigma$) were similar to northern hemispheric background concentrations (1.5–2.0 ng m^{-3}; Lamborg et al., 2002: Schroeder and Munthe, 1998) except for a few, less than 2-h long Hg-elevated pulses (Figs. 2 and 3; Table 3). The monthly coefficient of variation ($\sigma/\bar{x}$) for the Hg$^{\circ}$ concentration data at WB was low (10.2–20.0%) demonstrating that Hg$^{\circ}$ exhibited minimal temporal variability during the study period. Relatively stable concentrations of Hg$^{\circ}$ suggest that the global tropospheric pool is its likely source, rather than local input which would produce large variations and frequent elevated concentrations (Engle et al., 2006).

Fine particulate Hg concentrations varied markedly on diel and seasonal time scales (Figs. 2 and 3), with the highest concentrations measured during January–March of 2006 (3.4 ± 4.9–4.9 ± 5.4 pg m^{-3}). With the exception of a few multi-hour peaks which suggest input from local and regional sources, Hg-$PM_{2.5}$ concentrations (2.7 ± 3.4 pg m^{-3}) for the WB site were typical of background areas (<20 pg m^{-3}; Mason and Sheu, 2002; Gabriel et al., 2005). Concentrations of RGM at the WB site were highest during April and May of 2005 (monthly averages $= 9.6 \pm 15.4$ and 6.1 ± 10.1 pg m^{-3}, respectively) and were lowest in July of 2005 (monthly averages $= 1.9 \pm 3.2$ pg m^{-3}) and May of 2006 (1.5 ± 2.5 pg m^{-3}). Reactive gaseous Hg concentrations at the WB site (4.0 ± 7.5 pg m^{-3}) followed a diel pattern of low concentrations at night,

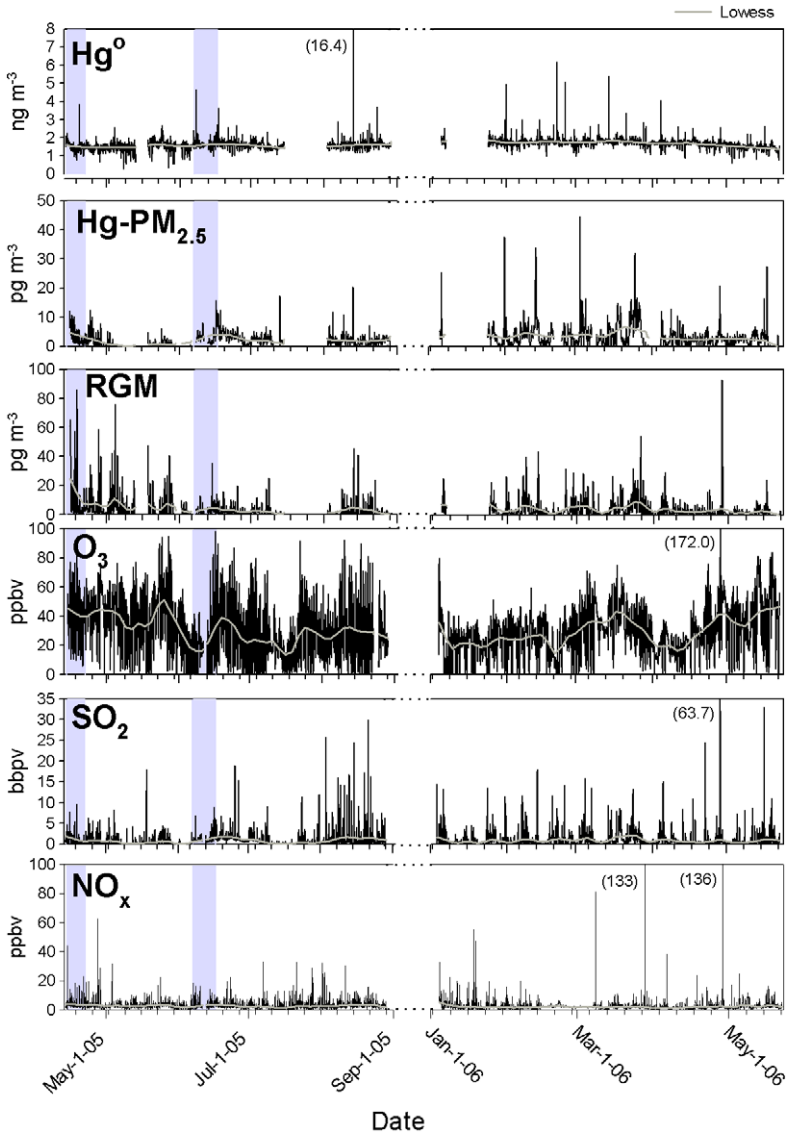

Fig. 2. Atmospheric Hg speciation and air quality results from the USGS Mobile Mercury Laboratory trailer in Weeks Bay, Alabama for 2005 (left) and 2006 (right). The gray boxes denote periods when aerosol sampling was completed. Lowess smoothing trend line shown in gray. Tics along the *x*-axis denote start of each Monday. Numbers in parentheses indicate maximum concentration of peaks which go off scale.

increasing in mid-morning to a midday maximum (up to 92.7 pg m^{-3}), then decreasing into the evening (Fig. 3). Midday maximum RGM concentrations at WB generally exceeded those for inland areas of southeastern USA and other background locations (<25 pg m^{-3}; Mason and Sheu, 2002; Gabriel et al., 2005; Edgerton et al., 2006; Valente et al., 2007). Although the daily maximum RGM concentration varied, the diel pattern was observed nearly every day. Similar diel patterns have been observed at urban, open ocean, coastal and arctic sites (Lindberg et al., 2002; Malcolm et al., 2003; Laurier and Mason, 2007; Liu et al., 2007).

Annual comparisons of concentration data for the three Hg species indicate that Hg° and Hg-$PM_{2.5}$ concentrations for 2006 were greater than those for 2005 ($p < 0.05$). Conversely, RGM concentrations were statistically greater in 2005 than in 2006 (Table 3), though differences are small relative to the detection limits and replication of the analytical methods. It is important to point out that comparison of results for 2005 vs. 2006, reflects not

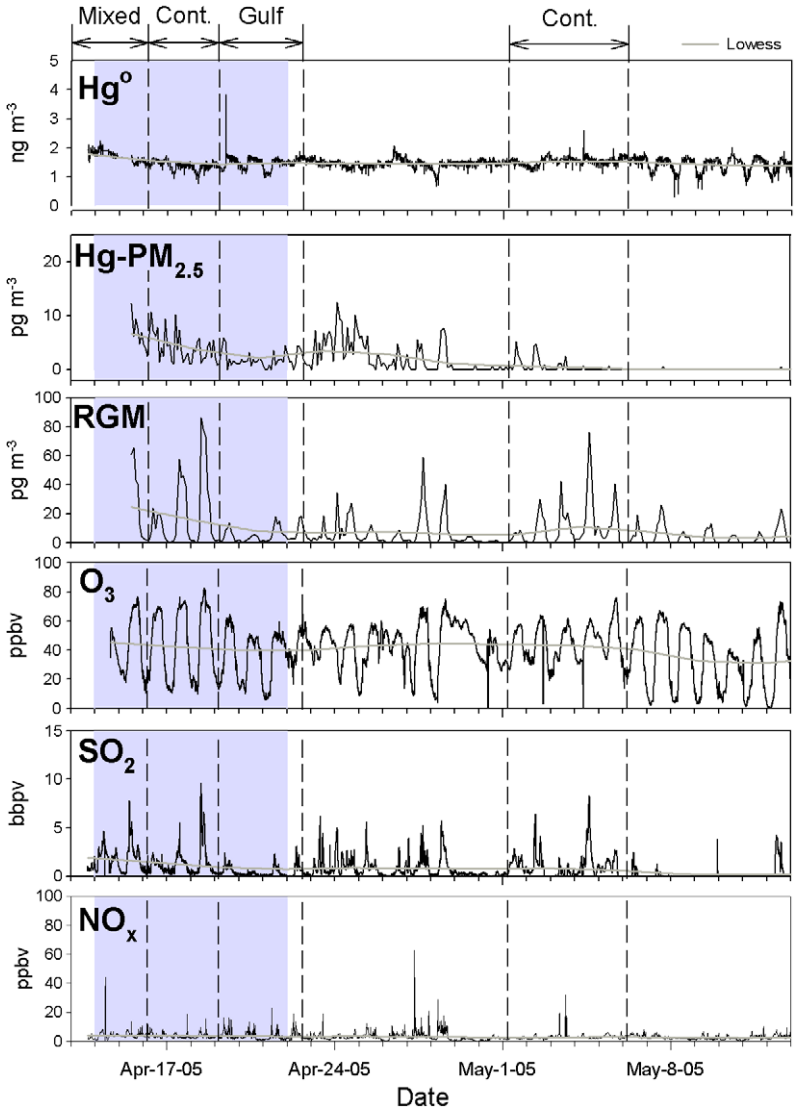

Fig. 3. Atmospheric Hg speciation and air quality results from the USGS Mobile Mercury Laboratory trailer in Weeks Bay, Alabama from April 15 to May 15, 2005. The gray box denotes a period when aerosol sampling was completed. Vertical dashed lines denote consistent patterns of >72-h long consecutive modeled air mass trajectories from a common source area (continental vs. Gulf vs. mixed), which are labeled at the top of the figure. Lowess smoothing trend line shown in gray. Tics along the *x*-axis denote start of each day. Cont. = continental.

only a difference in calendar year but also in season; the 2005 data were primarily collected during the summer and fall while those from 2006 are generally from winter and spring (see Table 4).

Ozone concentrations at the WB site were typical for the central Gulf Coast region and were elevated relative to data from remote areas (10–40 ppbv; Seinfeld and Pandis, 2006). Afternoon maximum values typically reached 60-80 ppbv during the warmer months and the data followed a diel pattern, typical of O_3 (Figs. 2 and 3). Like RGM, short-lived peaks of elevated O_3 concentrations (>60 ppbv) were more frequent in 2005 than in 2006 (Fig. 2). The kinetics of photochemical O_3 formation are driven by higher temperature and greater light intensity (Seinfeld and Pandis, 2006). Therefore higher O_3 concentrations would be expected during the summer and fall, compared to the winter and early spring, producing a pattern similar to that of Fig. 2.

The SO_2 concentration data exhibited short-lived (generally <2 h), non-repeating patterns of maxima which often exceeded typical background

Table 3
Summary of results from the USGS mobile mercury laboratory trailer at Weeks Bay, Alabama

Year	Month	Hg° (ng m^{-3})			Hg-$PM_{2.5}$ (pg m^{-3})			RGM (pg m^{-3})			O_3 (ppbv)			SO_2 (ppbv)		
		$\bar{x}$	σ	med.	$\bar{x}$	σ	med.	$\bar{x}$	σ	med.	$\bar{x}$	σ	med.	$\bar{x}$	σ	med.
2005	April	1.47	0.20	1.47	2.8	2.8	1.7	9.6	15.4	3.1	42.5	17.7	45.2	0.95	1.16	0.48
	May	1.55	0.26	1.57	0.5	1.0	0	6.1	10.1	1.0	39.2	20.8	39.8	0.45	1.06	0
	June	1.59	0.22	1.59	2.7	2.5	2.4	2.9	3.8	1.5	26.7	19.9	22.5	1.09	1.07	0.89
	July	1.53	0.16	1.50	1.9	1.9	1.7	1.9	3.2	0.8	23.8	17.5	19.2	0.42	0.95	0
	Aug	1.60	0.32	1.58	1.9	1.8	1.8	2.7	5.6	0.7	28.4	19.5	25.3	1.26	2.28	0.43
	All data	1.56	0.25	1.55	1.9	2.2	1.5	4.4	8.8	1.3*	31.2	20.5	29.0*	0.81	1.44	0.31
2006	January	1.80	0.21	1.77	3.4	4.9	2.8	4.5	5.7	2.4	22.0	12.8	23.0	0.69	1.20	0.20
	February	1.75	0.25	1.74	3.6	3.7	3.0	3.8	6.5	1.3	23.6	13.5	25.4	0.89	1.59	0.33
	March	1.76	0.18	1.76	4.9	5.4	3.2	5.0	6.9	1.8	35.6	15.1	36.1	1.27	1.66	0.56
	April	1.67	0.17	1.68	2.7	2.6	2.1	2.9	6.7	1.2	26.6	15.9	24.2	0.77	2.01	0.31
	May	1.46	0.18	1.47	2.2	2.5	2.0	1.5	2.5	0.6	39.2	19.0	41.7	0.69	1.38	0.21
	All Data	1.68	0.23	1.70**	3.4	4.1	2.6**	3.5	6.2	1.2	29.1	16.6	28.3	0.88	1.62	0.33**

$\bar{x}$ = mean, σ = standard deviation, med. = median.
* Indicates median concentration for 2005 significantly greater than for 2006 ($p < 0.05$).
** Indicates median concentration for 2006 significantly greater than for 2005 ($p < 0.05$).

concentrations (<10 ppbv; Biscoe et al., 1973). This pattern is indicative of localized plumes from local and regional point sources. Several periods of elevated RGM concentrations measured in August of 2005 corresponded with peaks of elevated SO_2 (Fig. 2).

Daytime (9AM–5PM) average Hg°, RGM, and Hg-$PM_{2.5}$ concentrations measured at the WB site correlated poorly (Hg° vs. RGM, Spearman $\rho = 0.09$; Hg° vs. Hg-$PM_{2.5}$, Spearman $\rho = 0.33$; RGM vs. Hg-$PM_{2.5}$, Spearman $\rho = 0.32$). The highly variable concentrations of Hg-$PM_{2.5}$ and RGM and their lack of correlation with Hg° data during the study (Figs. 2 and 3) suggests that the mixing ratio of these species was controlled by local sources and/or rapid exchange processes, rather than a regional or global background.

Correlation and multivariate regression analyses were also applied to better understand controls on the variability and average daytime concentration of RGM at the WB site. Data used in these analyses included daytime averages of air temperature, light intensity, wind speed, and concentrations of NO_x, SO_2 and O_3. Prior to analyses, the variables were individually transformed (e.g., log- and square root-transformed) as necessary to meet the requirements of the statistical methods. The 2005 RGM concentration data correlated most strongly ($p < 0.05$) with O_3, NO_x, light intensity and SO_2 (Spearman ρ values = 0.71, 0.57, 0.56, and 0.53, respectively; Fig. 4). Sulfur dioxide concentration ($\rho = 0.68$) is the only parameter that correlated strongly ($\rho > 0.5$ at $p < 0.05$) with the 2006 RGM data. All possible regression analysis, an iterative statistical routine which compares results for all permutations of variables (Hintze, 2005) was used to identify the strongest multivariate regression models with the fewest predictors for the 2005 and 2006 daytime average RGM data sets. Two models were generated for the 2005 RGM data: (1) O_3 concentration, the square root of light intensity, and square root of SO_2 concentration; and (2) the square of light intensity, the square root of SO_2 concentration, and the concentration of NO_x (adjusted $R^2 = 0.67$ for both models). Using the same technique for the 2006 daytime average data, a regression model based on the square root of SO_2 and the natural log of NO_x concentrations best predicted RGM concentration data (adjusted $R^2 = 0.49$).

Results from Kruskal–Wallis statistical tests indicated that for 7 of the 10 months of the study, average daytime RGM concentrations at WB were higher during periods of continental air mass trajectories than during Gulf regimes and were not statistically different than those corresponding with a mixed regime (Table 5). Average daytime RGM concentrations corresponding with mixed flow regimes were also greater than those measured during periods dominated by Gulf regimes for the 2006 data and the combined 2005 and 2006 data; this trend was not statistically present for any individual month of data. During periods dominated by Gulf regime backward air mass trajectories, the diel RGM pattern was present but maximum concentrations were greatly diminished relative to the other flow regimes (Fig. 3).

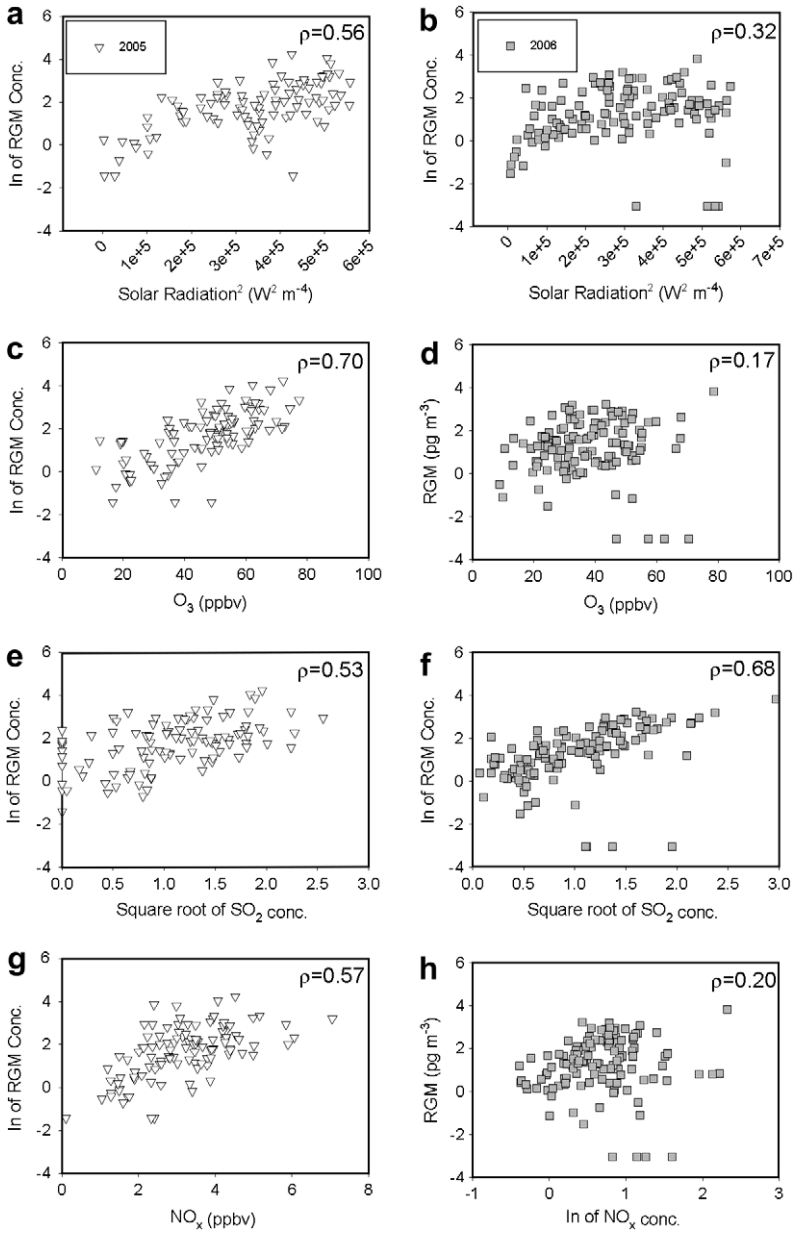

Fig. 4. Correlation of average daytime (9AM–5PM standard time) RGM data vs. solar radiation (a and b), O_3 (c and d), SO_2 (e and f), and NO_x (g and h) for 2005 and 2006. Data were mathematically transformed (i.e., natural log and square root) on a case by case basis to satisfy mathematical requirements of regression analyses. Spearman rank-based correlation coefficients (ρ) are also shown. All plots show statistically significant relationships ($p < 0.05$). This figure demonstrates significant differences in factors which correspond to RGM concentrations between the 2005 and 2006 data sets.

4.2. Total suspended particulate Hg results

Concentrations of Hg-TSP measured during this study were typical for those measured at background sites in terrestrial environments (<25 pg m^{-3}, Keeler et al., 1995; Table 6; Figs. 5 and 6). April 2005 Hg-TSP concentrations for the GS and WB sites ranged from 4.7 to 24.1 pg m^{-3} ($\bar{x} = 9.8$ and 13.8 pg m^{-3}, respectively) for the Low-Vol samples and 8.8–21.5 pg m^{-3} for the Hi-Vol samples ($\bar{x} = 12.4$ and 14.0 pg m^{-3}, respectively). Total suspended particulate Hg concentrations measured in June 2005 at GS and WB were not statistically different from April Low-Vol or

Table 4
Summary of meteorological data measured at Weeks Bay, Alabama

Year	Month	Air temp. (°C)			Light intens. (W m^{-2})			Windspeed (m s^{-1})			Total precip. (mm)
		$\bar{x}$	σ	med.	$\bar{x}$	σ	med.	$\bar{x}$	σ	med.	
2005	April	18.6	4.5	19.2	247	325	13	1.2	1.0	1.3	31
	May	22.5	4.7	23.1	258	324	43	0.9	0.8	0.9	121
	June	25.8	3.3	25.2	226	301	37	0.7	0.7	0.5	165
	July	27.3	3.2	27.0	224	298	38	0.9	1.0	0.7	65
	Aug	27.4	3.3	26.3	203	283	22	0.6	0.7	0.4	185
	All data	24.5	4.9	24.7	233	307	32	0.9	0.8	0.7	567
2006	January	13.5	5.8	14.7	120	199	0	1.5	1.2	1.4	61
	February	12.0	6.0	12.6	150	236	0	1.7	1.2	1.6	77
	March	16.5	5.8	17.8	208	288	2	1.7	1.2	1.8	26
	April	22.0	4.5	22.8	243	322	19	1.4	0.9	1.6	104
	May	22.5	4.2	23.4	258	326	45	1.2	0.9	1.4	137
	All data	17.4	6.8	18.3	197	285	3	1.5	1.1	1.6	405

$\bar{x}$ = mean, σ = standard deviation, med. = median.

Table 5
Percent frequency of backward air mass trajectory regimes and average ± standard deviation daytime RGM concentrations for 2005 and 2006

Year	Month	Continental		Gulf		Mixed		n
		Frequency	Daytime	Frequency	Daytime	Frequency	Daytime	
		(%)	RGM conc.	(%)	RGM conc.	(%)	RGM conc.	
2005	April	38	$27.5 \pm 19.8^{*}$	38	7.2 ± 5.4	25	30.3 ± 26.1	16
	May	25	$23.6 \pm 13.0^{*}$	54	10.7 ± 8.9	21	12.7 ± 8.1	24
	June	32	6.3 ± 3.2	48	4.4 ± 3.8	20	4.6 ± 1.0	25
	July	14	4.1 ± 5.8	64	2.5 ± 2.2	21	7.3 ± 4.3	14
	August	37	4.6 ± 4.2	48	7.8 ± 7.5	15	4.4 ± 2.6	27
	All data	30	12.7 ± 14.0	50	6.9 ± 6.9	20	11.8 ± 14.6	106
2006	January	60	$10.1 \pm 4.4^{*}$	30	1.0 ± 0.7	10	4.3 ± 0	10
	February	54	$12.3 \pm 8.9^{*}$	29	1.9 ± 0.9	18	5.9 ± 4.5	28
	March	39	$15.6 \pm 6.8^{*}$	45	5.7 ± 4.2	16	8.9 ± 7.1	31
	April	17	$9.4 \pm 5.9^{*}$	63	3.2 ± 1.8	20	11.3 ± 16.8	30
	May	33	$4.2 \pm 3.1^{*}$	62	1.7 ± 1.3	5	4.8 ± 0	21
	All data	38	$11.2 \pm 7.5^{*}$	48	3.2 ± 2.8	15	$8.1 \pm 9.9^{**}$	120
All 2005 & 2006 data		34%	$12.0 \pm 10.8^{*}$	49%	4.9 ± 5.5	17%	$10.1 \pm 12.5^{**}$	226

RGM concentration in pg m^{-3}.

* Indicates that the median daytime RGM concentrations associated with continental trajectories are significantly greater ($p < 0.05$; Kruskal–Wallis test) than those for Gulf trajectories.

** Indicates that the median daytime RGM concentrations associated with mixed trajectories are significantly greater ($p < 0.05$; Kruskal–Wallis test) than those for Gulf trajectories.

Hi-Vol data (Fig. 5); June Hg-TSP ranged from 4.6 to 16.3 pg m^{-3} ($\bar{x} = 8.4$ and 8.5 pg m^{-3}, respectively) for the Low-Vol samples and 6.2–53.7 pg m^{-3} for the Hi-Vol samples ($\bar{x} = 17.0$ and 12.8 pg m^{-3}, respectively). Samples from WB and GS also exhibited Hg-TSP concentrations that were not significantly different between daytime and nighttime sampling periods (data not shown). Concentrations of Low-Vol and Hi-Vol Hg-TSP samples collected at the inland SK site (sampled only in June) were significantly lower than those for the GS and WB sites (Low-Vol $\bar{x} = 5.5$ pg m^{-3}; Hi-Vol $\bar{x} = 7.9$ pg m^{-3}). This comparison, based on limited data, suggests that the WB and GS sites were located closer to the dominant sources of Hg-P than the SK site.

Hi-Vol Hg-TSP concentration data were significantly greater ($p < 0.05$) than for the Low-Vol samples (Fig. 5). This may be due to lower capture efficiency of coarse particles by the Low-Vol

Table 6
Summary of total suspended particulate Hg concentration data from the Low-Vol and Hi-Vol sampling events

Event	Site	$\bar{x}$	σ	med.	min.	max.	n
(a) Low-Vol data							
April 2005	GS	9.8	2.4	9.6	5.9	13.6	12
	WB	13.8	7.7	11.6	4.7	24.1	7
June 2005	GS	8.4	4.0	6.5	5.4	16.3	8
	WB	8.5	2.8	7.0	4.6	13.2	12
	SK	5.5	0.8	5.6	4.3	6.5	5
All Low-Vol data		9.7	5.0	8.6	4.3	24.1	44
(b) Hi-Vol data							
April 2005	GS	12.4	2.8	12.2	8.8	16.8	6
	WB	14.0	4.0	13.1	9.2	21.5	8
June 2005	GS	17.0	13.0	13.9	6.2	53.7	11
	WB	12.8	4.2	12.2	6.5	20.9	15
	SK	7.9	2.1	7.6	5.9	13.2	12
All Hi-Vol data		12.7	7.2	11.5	5.9	53.7	52

All data in units of pg m^{-3}. GS = Gulf Shores, WB = Weeks Bay, SK = Stockton. $\bar{x}$ = mean, σ = standard deviation, med. = median.

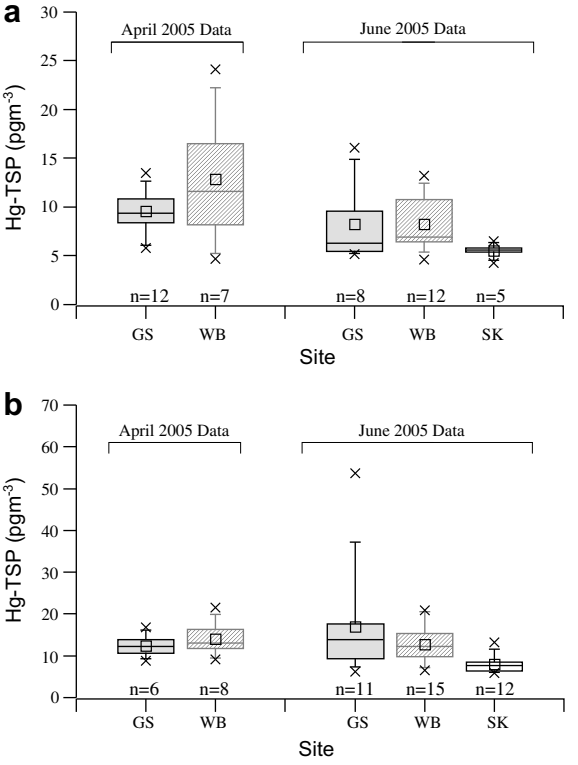

Fig. 5. Boxplots showing (a) Low-Vol and (b) Hi-Vol Hg-TSP concentrations from the Weeks Bay (WB), Gulf Shores (GS), and Stockton (SK) sites during the April and June 2005 aerosol samplings. Lower and upper bounds of the box indicate 25th and 75th percentiles; the horizontal line towards the middle of each box represent the median. The whiskers denote the 5th and 95th percentiles. Minimum and maximum data shown with X symbol. The squares denote the location of the arithmetic mean.

samplers as a result of their downward orientation and relatively low flow rate. The low inlet height of the Hi-Vol samplers (1.1 m vs. 2 m) may also allow for collection of large saltating particles in addition to atmospheric aerosols.

Tracers of coal-combustion, Se, and crustal sources, Al, (Wang et al., 2000), were measured in highest concentration (1.8 ± 1.4 and 114 ± 49.3 ng m^{-3}, respectively) in samples associated with the continental trajectory regime (Table 7), although many of the Se samples were near the detection limit of 1.0 ng m^{-3}. Samples corresponding to the Gulf regime exhibited the highest average concentration (167 ± 90.3 ng m^{-3}) of Mg, an indicator of sea salt aerosols (Graney et al., 2004), and the lowest average concentration of Se (1.0 ± 0.9 ng m^{-3}) and Al (73.4 ± 67.5 ng m^{-3}). Samples classified under the mixed trajectory regime, where contribution of both continental and marine-derived aerosols is predicted, contained intermediate concentrations of Se, Al and Mg (Table 7). The highest Low-Vol Hg-TSP concentrations were measured in samples collected during a mixed air mass regime (9.2 ± 3.4 pg m^{-3}) and the lowest in those corresponding to Gulf trajectories (6.9 ± 1.7 pg m^{-3}).

Air mass trajectory regime categorization of the Hi-Vol TSP samples produced results similar to those observed for the Low-Vol data (Table 7). The highest Cl^- concentrations (195 ± 235 ng m^{-3}) were measured in samples from a Gulf regime, consistent with derivation of Cl^- from sea salt aerosols. The highest SO_4^{2-} (945 ± 616 ng m^{-3}) and lowest average Cl^- concentration (31.0 ± 52.2) were found for samples collected during continental trajectory regimes, although the SO_4^{2-} concentrations were not significantly greater than those measured in mixed regime air masses (903 ± 304 ng m^{-3}). Interpretation of the SO_4^{2-} data is obfuscated because sulfate has both continental (e.g., SO_2 oxidation) and oceanic sources (e.g., sea salt and oxidation of dimethyl sulfide; Seinfeld and Pandis, 2006). The Hi-Vol Hg-TSP concentrations of samples corresponding to the three trajectories were similar (Table 7), although the highest concentrations were observed during daytime samples collected during mixed air mass regimes (18.1 ± 15.0 pg m^{-3}; data not shown).

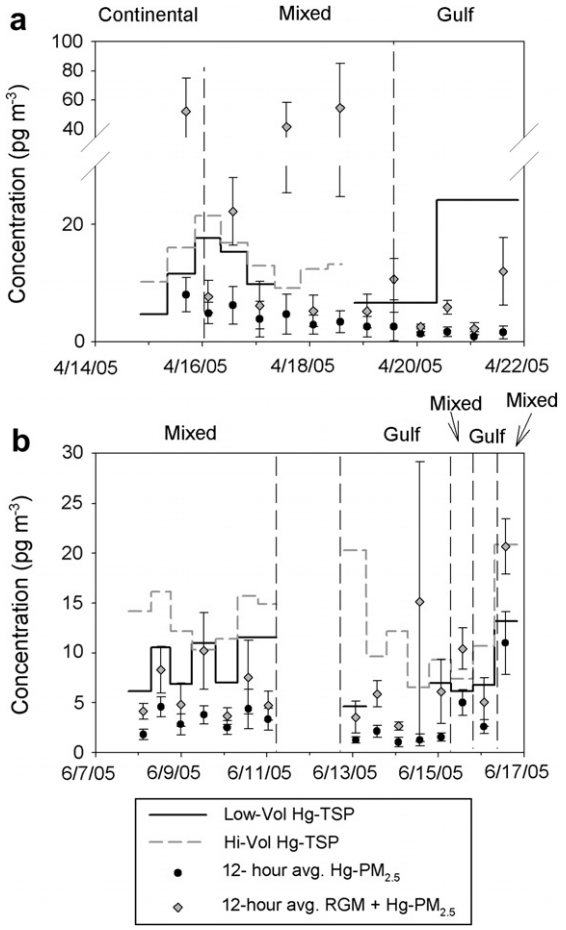

Fig. 6. Low-Vol and Hi-Vol Hg-TSP data from the Weeks Bay site for (a) April 2005 and (b) June 2005. Corresponding 12-h average fine particulate Hg (Hg-$PM_{2.5}$) and RGM+Hg-$PM_{2.5}$ data ± 1 standard deviation are also shown. Periods dominated by specific air mass trajectory regimes are labeled at the top of each plot and are separated by the vertical dashed lines. Note difference in scales between figures.

Reconnaissance scanning electron microscopy and microprobe analysis identified NaCl, Ca ± Mg-carbonate, aluminosilicate and phosphate phases on Hi-Vol filters which collected aerosols during Gulf-dominated regimes. Several of the NaCl particles identified on the filters were large, up to 20 μm diameter, suggesting that the source of these aerosols was local. Based on their chemical composition, their relative abundance, and modeled Gulf of Mexico source area, these large particles are most likely sea salt aerosols. Phases observed on filters employed during periods of continental air mass trajectories include aluminosilicate, Ca-sulfate, carbonate, quartz, and Fe-oxide particles.

Table 7
Results from sorting of aerosol data into air mass trajectory regimes

Data	Stat.	Continental	Gulf	Mixed
(a) Low-Vol data				
Hg-TSP	$\bar{x}$	8.2	6.9	9.2
	σ	3.5	1.7	3.4
	med.	6.5	6.3	8.9
Se	$\bar{x}$	1.8	1.0	1.5
	σ	1.4	0.9	0.7
	med.	1.4	0.5	1.5
Al	$\bar{x}$	114	73.4	99.3
	σ	49.3	62.6	80
	med.	90.9	67.5	87.6
Mg	$\bar{x}$	72.3	167	102
	σ	32.9	90.3	51.9
	med.	81.6	148	94
	n	9	10	16
(b) Hi-Vol data				
Hg-TSP	$\bar{x}$	11.9	12.5	13.8
	σ	4.9	4.0	10.6
	med.	10.2	11.8	11.8
Cl^-	$\bar{x}$	31.0	195	84.1
	σ	52.2	235	135
	med.	13.5	109	38.0
SO_4^{2-}	$\bar{x}$	945	640	903
	σ	616	141	304
	med.	842	629	823
	n	14	14	18

All units are ng m^{-3} except Hg-TSP (pg m^{-3}). $\bar{x}$ = mean, σ = standard deviation, med. = median.

Mercury was too low in concentration to be measured in any of the samples during microbeam analysis.

4.3. Size distribution of particulate Hg

At the WB site, one Hi-Vol sampler and one Low-Vol Hg-TSP sampler were collocated with the atmospheric Hg speciation system that provided Hg-$PM_{2.5}$ results (Fig. 6). For samples from 19 of 22 12-h Low-Vol sampling periods and for all of the Hi-Vol sampling periods, Hg-TSP concentrations exceeded 12-h average $\bar{x} + \sigma$ Hg-$PM_{2.5}$ concentrations ($p < 0.05$). These initial comparisons suggest that a significant fraction of Hg-P was bound to coarse particles. This finding must be taken cautiously because gas-to-particle transfer of Hg onto previously collected aerosols can cause positive artifacts (Landis et al., 2002; Lynam and Keeler, 2002), to undenuded aerosol samples (i.e., the Low-Vol TSP and Hi-Vol TSP samples; not the Hg-$PM_{2.5}$

data) especially during periods of higher RGM concentrations (>50 pg m^{-3}). Accounting for a worse-case scenario of this positive artifact (i.e., 100% of RGM collection on the filters shown as the sum of 12-h average RGM + Hg-$PM_{2.5}$ ± one standard deviation in Fig. 6), Hg-TSP concentrations for this limited data set exceeded 12-h average RGM + Hg-$PM_{2.5}$ in roughly 75% of the sampling periods. This statistically significant difference in Hg-P concentration (35 ± 29% by mass, max = 91% assuming minimal sampling artifacts) can be attributed to Hg-bearing coarse particles (>$PM_{2.5}$) that were not sampled by the atmospheric Hg speciation system due to sampler inlet limitations. In the remaining 25% of the data, Hg-TSP concentrations were lower than RGM + Hg-$PM_{2.5}$ concentrations ($p < 0.05$), indicating that RGM uptake on the filters was less than 100% (Fig. 6).

Negative Hg-P artifacts for samples for a similar coastal environment in Florida collected over a period of more than 4 h were recently demonstrated by Malcolm and Keeler (2007). Given the similar warm coastal settings for these two study areas, the Hg-TSP concentrations presented in this study may also have been subjected to negative artifacts, and would represent minimum values.

A second method of investigating the size distribution of Hg-P used collocated atmospheric Hg speciation system units at the OLF site (Table 2). Precision experiments to compare results with two analyzers using $PM_{2.5}$ inlets, showed that Hg°, Hg-$PM_{2.5}$ and RGM concentrations were generally not statistically different (Wilcoxon sign rank test, $p < 0.05$) within the range of analytical uncertainty (Hg° = <10%, RGM and Hg-P = 15–20%; Schroeder et al., 1995; Landis et al., 2002; Malcolm and Keeler, 2007). During the TSP and PM_{10} experiments, mean particulate Hg concentrations were statistically higher (on average 3.0–4.6 pg m^{-3}; 187–201%) on the collocated instrument (TSP or PM_{10} inlet) than the primary instrument ($PM_{2.5}$ inlet). The average fraction of Hg-P bound to the coarse particles (67% and 65% for TSP and PM_{10} experiments, respectively) was calculated as the difference between average Hg-P concentrations using the $PM_{2.5}$ and TSP or PM_{10} inlets divided by the average Hg-P concentration using the TSP or PM_{10} inlet configuration. It should be noted that these are short-term experiments and that results may or may not reflect annual average concentrations of Hg-P in the TSP or PM_{10} size ranges.

5. Discussion

As discussed, Hg speciation data results for the WB site suggest that Hg° concentrations were controlled by the global tropospheric pool, while Hg-$PM_{2.5}$ and RGM concentrations were predominantly influenced by local processes. The RGM concentrations at the WB site followed a diel pattern, which is indicative of rapid formation or deposition/destruction mechanisms, especially during periods dominated by continental and mixed flow regimes (Figs. 2 and 3). The diel RGM concentration patterns observed during Gulf trajectory regimes were of smaller magnitude, typically with maximum values at background levels (<25 pg m^{-3}; Mason and Sheu, 2002; Landis et al., 2004; Gabriel et al., 2005) suggesting that unpolluted air from the Gulf of Mexico was not a primary source of onshore RGM. This finding agrees with data for other coastal sites (Malcolm et al., 2003; Landis et al., 2004). Maximum daytime RGM concentrations at (up to 92.7 pg m^{-3}) WB were much greater than those observed at other rural, inland sites in southeastern USA, which exhibit background concentrations (Gabriel et al., 2005; Valente et al., 2007).

Peak daytime average RGM concentrations (>20 pg m^{-3}) were associated with two sets of physical and meteorological conditions. The highest RGM concentrations generally corresponded with an elevated O_3 (>55 ppbv) and high light intensity (>500 W m^{-2}) period in April and May of 2005 (Figs. 2–4). Mixed and continental air mass trajectories dominated this period (Table 5). Regression analyses of the 2005 data indicate that O_3, light intensity, and SO_2 best predicted average daytime RGM concentrations. A set of lower but still elevated RGM peaks (~20–30 pg m^{-3}) in January-March, 2006 correlated with SO_2 during periods of lower O_3 (30–55 ppbv), dominated by continental air mass trajectories (Figs. 2 and 4; Table 5).

There are three potential sources of the above background concentrations of RGM at the WB site: (1) direct emission of RGM from local sources, (2) oxidation of Hg° by anthropogenic and/or naturally-occurring atmospheric oxidants; and (3) influx of RGM-enriched air from the free troposphere into the boundary layer (Swartzendruber et al., 2006; Laurier and Mason, 2007). The first mechanism is supported by correspondence of high RGM concentration events, during certain periods, with peak concentrations of contaminants directly emitted from terrestrial sources (SO_2 and NO_x) and

continental/mixed trajectories (Figs. 2–4). However, poor correlation between RGM and co-emitted Hg species (i.e., Hg° and Hg-$PM_{2.5}$) during these events (Fig. 2) and the absence of irregular pulses typical of point source plumes (Fig. 3) suggests that direct emissions from terrestrial Hg point sources themselves were not the primary RGM source (Laurier and Mason, 2007). In the case of the latter mechanism, maximum RGM concentrations would be expected when boundary layer heights were at their highest, when input of free tropospheric air masses was greatest. However, correlation between average daytime RGM concentrations and modeled boundary layer heights from HYSPLIT was poor ($\rho = 0.22$; data not shown). The strong diel pattern of RGM concentrations is typical of other photochemically formed species, such as HO_2 (Seinfeld and Pandis, 2006) and during certain periods, such as 2005, RGM concentrations correlated well with O_3, a pervasive atmospheric oxidant which controls the concentration of other reactive species and oxidants (Sillman, 2005). This cursory evaluation suggests that photochemical oxidation of Hg° is likely the dominant source of elevated RGM during the study period.

The near background concentration and weak diel pattern of RGM corresponding to Gulf flow regimes, presented in this and other coastal atmospheric Hg speciation studies (Malcolm et al., 2003; Laurier and Mason, 2007), suggest that oxidation mechanisms attributed to RGM formation in the open ocean (e.g., halogen radicals; Hedgecock et al., 2003, 2005; Calvert and Lindberg, 2003) may be negligible in the near-shore marine boundary layer along the east coast of the United States. Oxidants more typically attributed to terrestrial RGM formation, such as $OH^{\cdot}$ and O_3, are seemingly better dominant Hg° photooxidation candidates in these coastal study areas (Lynam and Keeler, 2005). It is unclear if and how these reactions may be enhanced in the near-shore atmospheric environment relative to inland sites, which exhibit lower RGM concentrations (Gabriel et al., 2005; Valente et al., 2007).

Comparison of limited Hg-TSP filter data with Hg-$PM_{2.5}$ concentrations measured by the atmospheric Hg speciation unit at the WB site indicated that a significant fraction of particulate Hg was likely bound to coarse (>2.5 μm) particles. Similar results at the OLF site were found using an independent method which compared corresponding Hg-P concentrations from collocated atmospheric Hg speciation system units with different inlets (71% [no inlet] and 68% [PM_{10} inlet] of Hg-P bound to >2.5 μm diameter particles). Statistically lower Hi-Vol and Low-Vol Hg-TSP concentrations (on average 2.9–9.1 pg m^{-3} or 35–54%) were measured at the SK site, which is further inland and proximal to terrestrial point sources, than at the WB and GS sites (Table 6; Fig. 5). Results from this limited dataset suggest that proximity to the near-shore environment produced higher Hg-TSP concentrations.

Cursory electron microprobe examination of the Hi-Vol filters identified NaCl particles, presumably sea salt aerosols, on several samples collected during Gulf and mixed air mass regimes. The presence of these particles combined with elevated concentrations of RGM at the study site and the affinity of RGM for NaCl substrates (Rutter and Schauer, 2007), suggests that a fraction of coarse Hg-P at the WB site consisted of RGM sequestered by sea salt aerosols (Malcolm et al., 2003; Selin et al., 2007). However, additional work is required to demonstrate whether RGM uptake by sea salt aerosols was occurring.

The presence of Hg bound to large aerosols, such as sea salts, is significant because settling velocities are proportional to the square of the particle diameter (Seinfeld and Pandis, 2006). Thus, coarse particles (>5 μm) have been shown to dominate dry particulate deposition fluxes of trace elements (Holsen et al., 1993). Previous speciation studies, which relied only on atmospheric Hg speciation system Hg-$PM_{2.5}$ measurements, may underestimate particulate Hg concentrations, and thus dry deposition, in marine and coastal settings. Additional work is required to better understand the origin, seasonality, and impact of course particulate Hg in coastal settings.

6. Summary

The data presented in this paper characterized concentrations of atmospheric Hg species along the central Gulf Coast region of the United States. Concentrations of Hg° and Hg-P in the study area were typical of background sites; RGM data followed a diel pattern and with midday above-background maximum concentrations up to 92.7 pg m^{-3}. The source of the diel pattern and the mid-day maximum concentrations of RGM was likely photochemical oxidation of Hg° by naturally occurring and/or anthropogenic oxidants.

Additional investigation is required to better understand the role of coastal meteorology and near-shore terrestrial Hg and oxidant sources on RGM production and cycling.

Limited data from the WB and OLF sites suggest that a significant fraction of Hg-P was bound to coarse particles. A potential source of the coarse Hg-P includes uptake of RGM by sea salt aerosols, which were observed on filters collected during mixed and Gulf trajectory regimes. High annual precipitation tied with potential scavenging of Hg-P bound to soluble particles and RGM by water droplets during precipitation events may in part account for elevated Hg deposition rates along the US Gulf Coast region (up to 27 $\mu g\ m^{-2}\ a^{-1}$, Mercury Deposition Network, 2006); however more work is needed to investigate these hypotheses and to determine the magnitude and role of dry deposition.

An understanding of atmospheric Hg dynamics for the Gulf Coast region has potential implications for assessing the impact of natural and anthropogenic Hg sources to the environment. Further investigations are currently being conducted at additional coastal sites in the eastern USA. It is hoped that this on-going research will provide valuable information on the potential effects of placing future Hg sources in near-shore environments and the direct impacts of atmospheric Hg cycling on coastal ecosystems.

Acknowledgements

The authors acknowledge support for this study from the USGS Toxic Substances Hydrology Program, the DOI Landscapes Program, and the USGS Mendenhall Postdoctoral Fellowship Program. The authors also thank Mae Gustin (University of Nevada, Reno), William Cannon (USGS), and two anonymous reviewers for providing insightful comments on this manuscript. Alan Gertler (Desert Research Institute) and Jamie Schauer (University of Wisconsin, Madison) provided equipment for TSP sampling and input on sampling methods, which greatly improved the quality of the research. Mike Shelton and Scott Phipps of Weeks Bay National Estuarine Research Reserve provided invaluable assistance including access to the site and their facilities. Jamey McCord analyzed the trace element filters at the USGS Central Energy Team Labs in Denver, Colorado. Margo Corum provided IC analysis for anions on Hi-Vol filters at the USGS Biogeochemistry Laboratory in Reston, Virginia.

Disclaimer. Use of brand or trade names does not imply USGS endorsement.

References

Biscoe, P.V., Unsworth, M.H., Pinckney, H.R., 1973. The effects of low concentrations of sulphur dioxide on stomatal behaviour in *Vicia Faba*. New Phytol. 72, 1299–1306.

Branfireun, B.A., Krabbenhoft, D.P., Hintelmann, H., Hunt, R.J., Hurley, J.P., Rudd, J.W.M., 2005. Speciation and transport of newly deposited mercury in a boreal forest wetland: a stable mercury isotope approach. Water Resour. Res. 41, W06016. doi:10.1029/2004WR003219.

Calvert, J.G., Lindberg, S.E., 2003. A modeling study of the mechanism of the halogen-ozone-mercury homogeneous reactions in the troposphere during the polar spring. Atmos. Environ. 37, 4467–4481.

Calvert, J.G., Lindberg, S.E., 2005. Mechanisms of mercury removal by O_3 and OH in the atmosphere. Atmos. Environ. 39, 3355–3367.

Dvonch, J.T., Graney, J.R., Marsik, F.J., Keeler, G.J., Stevens, R.K., 1998. An investigation of source-receptor relationships for mercury in south Florida using event precipitation data. Sci. Total Environ. 213, 95–108.

Edgerton, E., Hartsell, B., Jansen, J., 2006. Mercury speciation in coal-fired power plant plumes observed at three surface sites in the Southeastern US. Environ. Sci. Technol. 40, 4563–4570.

Engle, M.A., Gustin, M.S., Goff, F., Counce, D.A., Janik, C.J., Bergfeld, D., Rytuba, J.J., 2006. Atmospheric mercury emissions from substrates and fumaroles associated with three hydrothermal systems in the western United States. J. Geophys. Res. 111, D17304. doi:10.1029/2005JD006563.

Ferrara, R., Mazzolai, B., Lanzillotta, E., Nucaro, E., Pirrone, N., 2000. Volcanoes as emission sources of atmospheric mercury in the Mediterranean basin. Sci. Total Environ. 259, 115–121.

Fitzgerald, W., Lamborg, C., 2005. Geochemistry of mercury in the environment. In: Holland, H., Turekian, K. (Eds.), Environmental Geochemistry, Treatise on Geochemistry, vol. 9. Elsevier, pp. 107–148 (Chapter 4).

Fitzgerald, W., Engstrom, D., Mason, R., Nater, E., 1998. The case for atmospheric mercury contamination in remote areas. Environ. Sci. Technol. 32, 1–7.

Friedli, H.R., Radke, L.F., Prescott, R., Hobbs, P.V., Sinha, P., 2003. Mercury emissions from the August 2001 wildfires in Washington State and an agricultural waste fire in Oregon and atmospheric mercury budget estimates. Global Biogeochem. Cycles 17, 1039. doi:10.1029/2002GB001972.

Gabriel, M.C., Williamson, D.G., Brooks, S., Lindberg, S., 2005. Atmospheric speciation of mercury in two contrasting Southeastern US airsheds. Atmos. Environ. 39, 4947–4958.

Garbarino, J.R., Kanagy, L.K., Cree, M.E., 2006. Determination of elements in natural-water, biota, sediment, and soil samples using collision/reaction cell inductively coupled plasma-mass spectrometry. US Geological Survey Techniques and Methods, Methods of the National Water Quality Laboratory, vol. 5. US Geol. Sur. (Chapter 1).

Graney, J.R., Dvonch, J.T., Keeler, G.J., 2004. Use of multi-element tracers to source apportion mercury in south Florida aerosols. Atmos. Environ. 38, 1715–1726.

Guentzel, J.L., Landing, W.M., Gill, G.A., Pollman, C.D., 1998. Mercury and major ions in rainfall, throughfall, and foliage from the Florida Everglades. Sci. Total Environ. 213, 43–51.

Guentzel, J., Landing, W., Gill, G., Pollman, C., 2001. Processes influencing rainfall deposition of mercury in Florida. Environ. Sci. Technol. 35, 863–873.

Gustin, M.S., 2003. Are mercury emissions from geologic sources significant? A status report. Sci. Total Environ. 304, 153–167.

Hanna, S.R., 1991. Characteristics of ozone episodes during SCCCAMP 1985. J. Appl. Meteorol. 30, 534–550.

Hedgecock, I.M., Pirrone, N., Sprovieri, F., Pesenti, E., 2003. Reactive gaseous mercury in the marine boundary layer: Modelling and experimental evidence of its formation in the Mediterranean region. Atmos. Environ. 37 (Supp. 1), 41–49.

Hedgecock, I.M., Trunfio, G.A., Pirrone, N., Sprovieri, F., 2005. Mercury chemistry in the MBL: Mediterranean case and sensitivity studies using the AMCOTS (Atmospheric Mercury Chemistry over the Sea) model. Atmos. Environ. 39, 7217–7230.

Hines, N., Brezonik, P., 2007. Mercury inputs and outputs at a small lake in northern Minnesota. Biogeochemistry 84, 265–284.

Hintelmann, H., Harris, R., Heyes, A., Hurley, J., Kelly, C., Krabbenhoft, D., Lindberg, S., Rudd, J., Scott, K., St.Louis, V., 2002. Reactivity and mobility of new and old mercury deposition in a boreal forest ecosystem during the first year of the METAALICUS study. Environ. Sci. Technol. 36, 5034–5040.

Hintze, J.L., 2005. NCSS 2004 Statistical Software User's Guide.

Holsen, T.M., Noll, K.E., Fang, G.C., Lee, W.J., Lin, J.M., Keeler, G.J., 1993. Dry deposition and particle size distributions measured during the Lake Michigan Urban Air Toxics Study. Environ. Sci. Technol. 27, 1327–1333.

Jaffe, D., Prestbo, E., Swartzendruber, P., Weiss-Penzias, P., Kato, S., Takami, A., Hatakeyama, S., Kajii, Y., 2005. Export of atmospheric mercury from Asia. Atmos. Environ. 39, 3029–3038.

Keeler, G., Glinsorn, G., Pirrone, N., 1995. Particulate mercury in the atmosphere: its significance, transport, transformation and sources. Water Air Soil Pollut. 80, 159–168.

Krabbenhoft, D., Gilmour, C., Orem, W., Aiken, G., 2004. Unraveling the complexities of mercury methylation in the Everglades: the use of mesocosms to test the effects of "new" mercury, sulfate, and dissolved organic carbon. Mater. Geoenviron. 51, 1150–1151.

Krabbenhoft, D.P., Branfireun, B.A., Heyes, A., 2005. Biogeochemical Cycles Affecting the Speciation and Transport of Mercury in the Environment, Short Course Series, vol. 34. Mineralogical Association of Canada, pp. 139–156 (Chapter 8).

Lamborg, C.H., Fitzgerald, W.F., O'Donnell, J., Torgersen, T., 2002. A non-steady-state compartmental model of global-scale mercury biogeochemistry with interhemispheric atmospheric gradients. Geochim. Cosmochim. Acta 66, 1105–1118.

Landis, M., Stevens, R., Schaedlich, F., Prestbo, E., 2002. Development and characterization of an annular denuder methodology for the measurement of divalent inorganic reactive gaseous mercury in ambient air. Environ. Sci. Technol. 36, 3000–3009.

Landis, M.S., Keeler, G.J., Al-Wali, K.I., Stevens, R.K., 2004. Divalent inorganic reactive gaseous mercury emissions from a mercury cell chlor-alkali plant and its impact on near-field atmospheric dry deposition. Atmos. Environ. 38, 613–622.

Laurier, F., Mason, R., 2007. Mercury concentration and speciation in the coastal and open ocean boundary layer. J. Geophys. Res. 112, D06302. doi:10.1029/2006JD007320.

Lindberg, S., Brooks, S., Lin, C.-J., Scott, K., Landis, M., Stevens, R., Goodsite, M., Richter, A., 2002. Dynamic oxidation of gaseous mercury in the Arctic troposphere at polar sunrise. Environ. Sci. Technol. 36, 1245–1256.

Liu, B., Keeler, G.J., Dvonch, J.T., Barres, J.A., Lynam, M.M., Marsik, F.J., Morgan, J.T., 2007. Temporal variability of mercury speciation in urban air. Atmos. Environ. 41, 1911–1923.

Lynam, M.M., Keeler, G.J., 2002. Comparison of methods for particulate phase mercury analysis: sampling and analysis. Anal. Bioanal. Chem. 374, 1009–1014.

Lynam, M., Keeler, G., 2005. Automated speciated mercury measurements in Michigan. Environ. Sci. Technol. 39, 9253–9262.

Malcolm, E.G., Keeler, G.J., 2007. Evidence for a sampling artifact for particulate-phase mercury in the marine atmosphere. Atmos. Environ. 41, 3352–3359.

Malcolm, E.G., Keeler, G.J., Landis, M.S., 2003. The effects of the coastal environment on the atmospheric mercury cycle. J. Geophys. Res. 108, 4357. doi:10.1029/2002JD003084.

Marsik, F.J., Keeler, G.J., Landis, M.S., 2007. The dry-deposition of speciated mercury to the Florida Everglades: measurements and modeling. Atmos. Environ. 41, 136–149.

Mason, R., Sheu, G.-R., 2002. Role of the ocean in the global mercury cycle. Global Biogeochem. Cycles 16, 1093. doi:10.1029/2001GB001440.

Mason, R.P., Fitzgerald, W.F., Morel, F.M.M., 1994. The biogeochemical cycling of elemental mercury: anthropogenic influences. Geochim. Cosmochim. Acta 58, 3191–3198.

Mercury Deposition Network, 2006. NADP Program Office, Illinois State Water Survey, 2204 Griffith Dr., Champaign, IL 61820. http://nadp.sws.uiuc.edu/mdn/.

Morel, F., Kraepiel, A., Amyot, M., 1998. The chemical cycle and bioaccumulation of mercury. Annu. Rev. Ecol. Syst. 29, 543–566.

Muller, R.A., 1977. A synoptic climatology for environmental baseline analysis: New Orleans. J. Appl. Meteor. 16, 20–33.

Ning, Z.H., Abdollahi, K., 2003. Gulf coast regional climate. In: Ning, Z.H., Turner, R.E., Doyle, T., Abdollahi, K. (Eds.), Gulf Coast Region: Findings of the Gulf Coast Regional Assessment. Gulf Coast Climate Change Assessment Council, pp. 79–82 (Chapter 5).

Olund, S.D., DeWild, J.F., Olson, M.L., Tate, M.T., 2004. Methods for the preparation and analysis of solids and suspended solids for total mercury. Laboratory Analysis, Book 5, Section A, Water Analysis. US Geol. Surv. (Chapter 8).

Pal, B., Ariya, P., 2004a. Gas-phase HO•-initiated reactions of elemental mercury: Kinetics, product studies, and atmospheric implications. Environ. Sci. Technol. 38, 5555–5566.

Pal, B., Ariya, P.A., 2004b. Studies of ozone initiated reactions of gaseous mercury: kinetics, product studies, and atmospheric implications. Phys. Chem. Chem. Phys. 6, 572–579.

Paterson, M.J., Blanchfield, P.J., Podemski, C., Hintelmann, H.H., Gilmour, C.C., Harris, R., Ogrinc, N., Rudd, J.W., Sandilands, K.A., 2006. Bioaccumulation of newly deposited mercury by fish and invertebrates: an enclosure study using stable mercury isotopes. Can. J. Fish. Aquat. Sci. 63, 2213–2224.

Poissant, L., Pilote, M., Xu, X., Zhang, H., Beauvais, C., 2004. Atmospheric mercury speciation and deposition in the Bay St. François wetlands. J. Geophys. Res. 109, D11301. doi:10.1029/2003JD004364.

Rogers, D.P., 1995. Coastal meteorology. Rev. Geophys. 33 (Supp. 1), 889–896.

Rutter, A., Schauer, J., 2007. The impact of aerosol composition on the particle to gas partitioning of reactive mercury. Environ. Sci. Technol. 41, 3934–3939.

Schroeder, W.H., Munthe, J., 1998. Atmospheric mercury – an overview. Atmos. Environ. 32, 809–822.

Schroeder, W.H., Keeler, G., Kock, H., Roussel, P., Schneeberger, D., Schaedlich, F., 1995. International field intercomparison of atmospheric mercury measurement methods. Water Air Soil Pollut. 80, 611–620.

Seigneur, C., Vijayaraghavan, K., Lohman, K., Karamchandani, P., Scott, C., 2004. Global source attribution for mercury deposition in the United States. Environ. Sci. Technol. 38, 555–569.

Seinfeld, J.H., Pandis, S.N., 2006. Atmospheric Chemistry and Physics, second ed. John Wiley & Sons Inc.

Selin, N.E., Jacob, D.J., Park, R.J., Yantosca, R.M., Strode, S., Jaeglé, J., Jaffe, D., 2007. Chemical cycling and deposition of atmospheric mercury: global constraints from observations. J. Geophys. Res. 112, D02308. doi:10.1029/2006JD007450.

Sheu, G.-R., Mason, R.P., 2004. An examination of the oxidation of elemental mercury in the presence of halide surfaces. J. Atmos. Chem. 48, 107–130.

Sillman, M., 2005. Tropospheric ozone and photochemical smog. In: Holland, H., Turekian, K. (Eds.), Environmental Geochemistry, Treatise on Geochemistry, vol. 9. Elsevier, pp. 407–431 (Chapter 11).

Sommar, J., Gardfeldt, K., Stromberg, D., Feng, X., 2001. A kinetic study of the gas-phase reaction between the hydroxyl radical and atomic mercury. Atmos. Environ. 35, 3049–3054.

Swartzendruber, P.C., Jaffe, D.A., Prestbo, E.M., Weiss-Penzias, P., Selin, N.E., Park, R., Jacob, D.J., Strode, S., Jaeglè, L., 2006. Observations of reactive gaseous mercury in the free troposphere at the Mount Bachelor Observatory. J. Geophys. Res. 111, D24301. doi:10.1029/2006JD007415.

Valente, R.J., Shea, C., LynnHumes, K., Tanner, R.L., 2007. Atmospheric mercury in the Great Smoky Mountains compared to regional and global levels. Atmos. Environ. 41, 1861–1873.

Wang, C., Zhu, W., Wang, Z., Guicherit, R., 2000. Rare earth elements and other metals in atmospheric particulate matter in the western part of the Netherlands. Water Air Soil Pollut. 121, 109–118.

Wängberg, I., Munthe, J., Ebinghaus, R., Gardfeldt, K., Iverfeldt, A., Sommar, J., 2003. Distribution of TPM in northern Europe. Sci. Total Environ. 304, 53–59.

Xu, X., Yang, X., Miller, D.R., Helble, J.J., Carley, R.J., 1999. Formulation of bi-directional atmosphere-surface exchanges of elemental mercury. Atmos. Environ. 33, 4345–4355.

Zillioux, E., Porcella, D., Benoit, J., 1993. Mercury cycling and effects in freshwater wetland ecosystems. Environ. Toxicol. Chem. 12, 2245–2264.